

Linear and nonlinear intraband optical absorption in (In,Ga)N spherical QD: effects of *In*-concentration, optical Intensity, size and impurity

HADDOU EL GHAZI^{a,b,*}, A. JORIO^a, I. ZORKANI^a

^aLPS Faculty of science, Dhar El Mehrez, BP 1796 Fes-Atlas, Morocco

^bSpecial mathematics, CPGE My Youssef, Rabat, Morocco

The linear, third-order nonlinear and total intrasubband optical absorption coefficients ACs of 1s-1p, 1p-1d and 1f-1d transitions with and without hydrogenic shallow-donor impurity in wurtzite (In,Ga)N/GaN spherical quantum dot (SQD) are reported. Incident optical intensity, QD radius and potential barrier effects are investigated. The calculations are performed within the framework of single band effective-mass approximation using a combination of Quantum Genetic Algorithm (QGA) and Hartree-Fock-Roothaan (HFR) method. Our results show that: (i) a critical value of the incident optical intensity is obtained which constitutes a turning point of two intensities behaviors and (ii) a significant blue shift of the resonant peaks of optical ACs is observed under the *In*-composition, the QD radius and the presence of the impurity.

(Received January 05, 2014; accepted November 13, 2014)

Keywords: Quantum Dot, Optical absorption, InGaN

1. Introduction

In the last decades, intense research is focused on optical and other physical properties of wide-band gap III-V nitrides, such GaN, AlN, InN and their ternary compounds, due to their extraordinary capacity and potential for device application. The immense advance of modern nanotechnology has given the opportunity to obtain the nanostructures with three-dimensional confinement of electrons called quantum dot (QD). These structures show an interesting behavior and play a significant role in microelectronic and optoelectronic. The atomic properties like discrete energy levels and shell structures are depicted in such structure. Therefore, the electronic structures, energy states, optical and other properties of one- and two-electrons in QDs have been commonly studied using different calculation methods [1-7].

The third-order nonlinear optical properties of low-dimensional semiconductor systems have attracted much attention for both theoretical researches and practical applications such infrared photo detectors, far-infrared laser amplifiers, optical memory technology, light emitting diode, high-speed electro-optical modulators and so on [8-19]. Liu et al. [9] have performed the calculation of linear and nonlinear optical intersubband absorption coefficients (ACs) and refractive index changes in cylindrical quantum well (CQWW). Using an approach which is a combination of Quantum Genetic Algorithm (QGA) procedure and Hartree-Fock Roothaan (HFR) method, the optical ACs for lowest energy states in GaAs QDs are reported by several authors [11-14]. Using the matrix diagonalization method, Sahin et al. [15] have investigated the hydrogenic impurity

effect on the third-order nonlinear optical properties of one- and two-electron SQD. Shao et al. [16] have investigated the effect of external applied electric field on the third-harmonic generations in cylindrical QDs. Incidentally; Zhang et al. [17] have examined the effects of incident optical intensity, QD radius and hydrogenic impurity on the linear and nonlinear optical properties of strained GaN/AlN QD. Recently, Kirak et al. [18] reported a detailed calculation of electric field influence on electronic properties in parabolic QDs. Also, they studied the linear and nonlinear optical ACs and the refractive index changes for 1s-1p and 1p-1d transitions using a variational method. To the best of our knowledge, all of the above mentioned works are focused on the lowest energy states between the ground ($l=0$) and the first excited ($l=1$).

In the present work, the effects of incident optical intensity, dot radius, hydrogenic impurity and potential barrier (*In*-fraction) on linear, nonlinear and total intrasubband ACs of 1s-1p, 1p-1d and 1d-1f transitions in (In,Ga)N/GaN SQDs are investigated.

2. Theoretical formalism

In this paper, the results are given in the effective units, i.e., the effective Rydberg energy $R^* = \frac{m^* e^4}{2\hbar^2 \epsilon_0^2}$ as

the unit of the energy and the effective Bohr radius $a^* = \frac{\epsilon_0 \hbar^2}{m^* e^2}$ as the unit of length. Within the framework

of single band effective-mass and the parabolic band approximations, the Hamiltonian of the electron in the presence of an on-center shallow-donor impurity in wurtzite $\text{In}_x\text{Ga}_{1-x}\text{N}$ SQD of radius R surrounded by GaN environment can be written as:

$$H = -\nabla^2 - \frac{2}{r} + V(r) \quad (1)$$

r is the electron-impurity distance and $V(r)$ is the finite potential barrier given as:

$$V(r) = \begin{cases} 0 & r \leq R \\ Q\Delta E_g(x) & \text{elsewhere} \end{cases} \quad (2)$$

$Q(=0.7)$ and ΔE_g are respectively the conduction band off-set parameter and the difference between the band gaps of GaN and $\text{In}_x\text{Ga}_{1-x}\text{N}$ which are the same as those used in Refs. [20].

To obtain the eigenvalues and eigenvectors of the time independent Schrödinger equation, we have adopted the method which is the combination of QGA and HFR procedures detailed in Refs. [1,2]. In the recent works, linear, third-order nonlinear and total ACs are given as [21-23]:

$$\alpha^{(1)}(\omega) = \omega \sqrt{\frac{\mu}{\varepsilon_r \varepsilon_0}} \frac{\hbar \Gamma_{if} |M_{fi}|^2 \rho}{(E_{fi} - \hbar \omega)^2 + (\hbar \Gamma_{if})^2} \quad (3)$$

$$\alpha^{(3)}(\omega, I) = -\omega \sqrt{\frac{\mu}{\varepsilon_r}} \left(\frac{I}{2\varepsilon_0 n_r c} \right) \frac{4\rho \hbar \Gamma_{if} |M_{fi}|^4}{(E_{fi} - \hbar \omega)^2 + (\hbar \Gamma_{if})^2}. \quad (4)$$

$$\left[1 - \frac{|M_{ff} - M_{ii}|^2}{4|M_{fi}|^2} \cdot \frac{3E_{fi}^2 - 4\hbar\omega E_{fi} + \hbar^2(\omega^2 - \Gamma_{fi}^2)}{E_{fi}^2 + (\hbar\Gamma_{fi})^2} \right] \alpha(\omega, I) = \alpha^{(1)}(\omega) + \alpha^{(3)}(\omega, I) \quad (5)$$

Notice that ρ is the electron density in SQD which is given as $\rho = N/V_{QD}$, N is the number of electrons in QD and V_{QD} is the volume of the QD. I is the intensity of incident optical radiation, $\hbar\omega$ is the incident photon energy, μ is the permeability of the system, Γ_{fi} is the non-diagonal matrix element ($i \neq f$) called as relaxation rate of final and initial states which is the inverse of relaxation time τ_{fi} , $n_r = \sqrt{\varepsilon_r}$ represents the relative refractive index of the semiconductor, c is the speed of the light in vacuum and ε_0 is the static electrical permittivity of the vacuum. The difference of the energy

between the final and initial states is given as $E_{fi} = E_f - E_i$. As seen from Eq. 5, since the third-order nonlinear optical AC is negative and is proportional to the incident optical intensity (Eq. 4), the total AC decreases as the incident intensity increases.

For an incident electromagnetic radiation polarized along z-axis and within electric dipole approximation, the dipole transition matrix element between i_{th} (lower) and f_{th} (upper) states is given as $M_{fi} = e \langle \psi_f | r \cos \theta | \psi_i \rangle$. This latter is very important parameter to obtain different optical properties related to electronic transitions. To perform our calculation related to electric dipole matrix element, we have used the eigenvalues and the wavefunctions reported by Özmen et al. [11]. Taking into account of the spherical symmetry of the system, the dipole transitions are allowed only between states satisfying the selection rule $\Delta l = \pm 1$, l is the angular momentum quantum number.

Notice that in low-dimensional quantum mechanical systems; photoabsorption process can be defined as an optical intrasubband transition occurred from a lower state (initial) to an upper state (final).

3. Results and discussion

The linear, third-order nonlinear and total intersubband optical ACs are computed in $\text{In}_x\text{Ga}_{1-x}\text{N}/\text{GaN}$ spherical QD for both cases, with and without the impurity. For well (barrier) region, we have used the material parameters of $\text{In}_x\text{Ga}_{1-x}\text{N}$ (GaN) since their physical parameters are well known and are used in our previous work [24,25]. The difference between the band gaps of GaN and $\text{In}_x\text{Ga}_{1-x}\text{N}$ is $\Delta E_g(x) = (6.44x - 3.8x^2)$. The effective dielectric constant and the effective-mass in ternary alloy are given respectively as $\varepsilon_r(x) = (9.8 + 3.9x)$ and $m^*(x) = (0.19 - 0.09x)m_0$ while m_0 is the free electron mass. Using the above given parameters for $x = 0.2$, one can obtain respectively a^* and R^* as 2.80 nm and 26.65 meV.

The results of our calculations are presented in Figs. 1-3. Fig. 1 displays the square of the electric dipole transition matrix element between initial and final states. As can be seen, the square of dipole matrix elements increases versus the SQD radius. The increase of 1d-1f transition is more significant than those of 1p-1d and 1s-1p. It is shown that for all transitions, $|M_{if}|$ increases as a function of the dot radius for finally to converge to the bulk results corresponding (In,Ga)N semiconductor material. It is interesting to mention that the saturation regime depends on the transition.

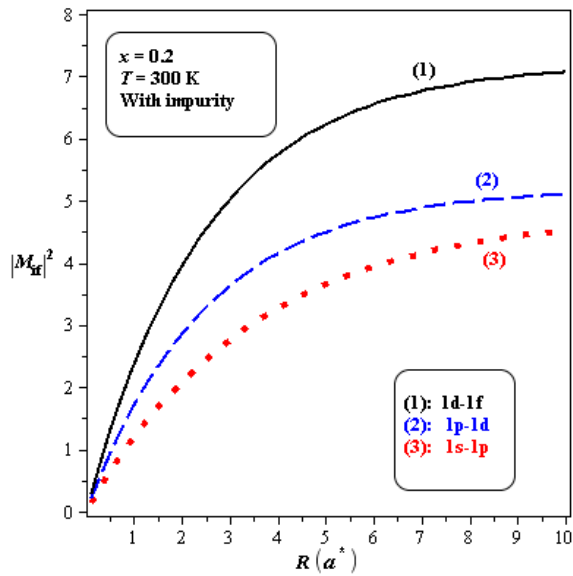


Fig. 1. The Square of electric dipole matrix element (a.u) of QD with an on-center hydrogenic impurity as a function of the dot radius. (a.u: arbitrary unit).

Fig. 2 shows the total optical ACs versus the incident photon energy ($\hbar\omega$) in both cases with and without the presence of an on-center impurity for three different values of the incident optical intensity. Without excitation ($I = 0 \text{ MW.m}^{-2}$), the third-order nonlinear AC is equal to zero and then, the total AC is equal to the linear contribution. For $I \neq 0$, the total AC decreases according to the incident intensity due to the nonlinear contribution. Therefore, as the intensity increases the nonlinear AC should be taken into account. It appears from Fig. 2 that the maximum of the AC decreases versus the incident intensity. Notice that a critical value of the incident intensity, called as a turning point, is obtained. For the incident intensity greater than a critical value (I_c) corresponding to the saturation regime, a collapse at the center of the total AC peaks is observed, i.e., two peaks appeared due to the nonlinear term. Notice that, the saturation regime depends on the transition and the impurity. Without the impurity, it is obtained respectively at 52 MW.m^{-2} , 50 MW.m^{-2} and 47 MW.m^{-2} for 1s-1p, 1p-1d and 1d-1f transitions. For the case corresponding to the presence of the impurity, it is obtained around 53 MW.m^{-2} for 1s-1p, 52 MW.m^{-2} for 1p-1d and 49 MW.m^{-2} for 1d-1f. It is interesting to mention that under the incident excitation no shift of the resonance peak position is observed. However, it is clearly from the same figure that the presence of the impurity causes a significant blue shift of the AC peaks. This shift is more important in transitions between lower levels, i.e. it is about $1.3 R^*$ for 1s-1p, $0.9 R^*$ for 1p-1d and $0.6 R^*$ for 1d-1f. This effect can be explained by the fact that the electron is more localized near the impurity and then is more attracted for 1s than 1p and 1d.

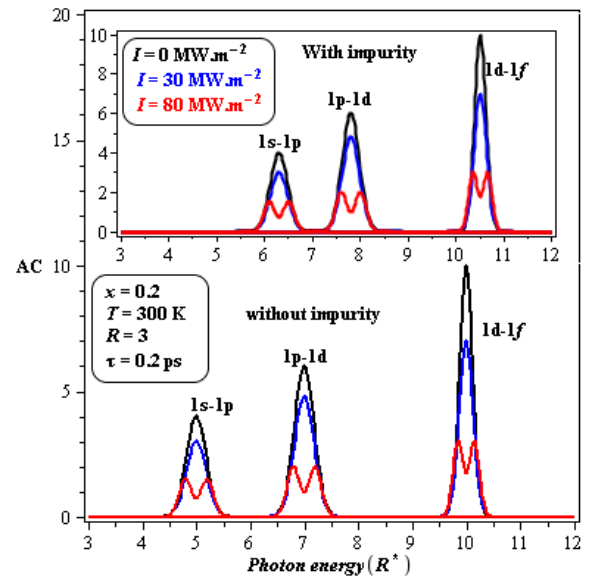


Fig. 2. The total optical ACs (10^4 cm^{-1}) for 1s-1p, 1p-1d and 1d-1f transitions in $\text{In}_{0.2}\text{Ga}_{0.8}\text{N}$ SQD as a function of the incident photon energy. The effects of the incident optical intensity and the presence of the impurity are included.

The results regarding the effect of the confining potential (*In*-composition) on linear, third-order nonlinear and total optical ACs of 1s-1p, 1p-1d and 1d-1f transitions in $\text{In}_x\text{Ga}_{1-x}\text{N}$ SQD as a function of the incident photon energy are depicted in Fig.3. According to Eq. (2), the confining potential barrier increases when the *In*-concentration increases. It is equal to 274 meV, 500 meV and 720 meV for $x = 0.1$, $x = 0.2$ and $x = 0.3$ respectively. It is clear that in all cases, with and without impurity, the optical properties are strongly affected by changing the stoichiometric value. It can be noted that the linear ACs are increased with increasing x while the third-order nonlinear ACs are remarkably reduced due to their negative sign. Furthermore, the increase of the *In*-composition enhances the total ACs. The amplitudes of the optical ACs increase when going to the transitions between higher electronic energy states. This behavior can be attributed to the increase of the electronic transition matrix element with increasing x . As can be seen from the same figure, a significant displacement of the position of the ACs peaks toward higher energy range is observed. The blue shift is not the same and depends on the transition. The main factor responsible for such behavior is the wave-function dependence versus the *In*-concentration inside the dot, i.e., the electron wave-function is more strongly localized inside the dot which leads to large separation of the initial and final energy levels. This result is in good agreement with the finding results [8, 14, 26-30].

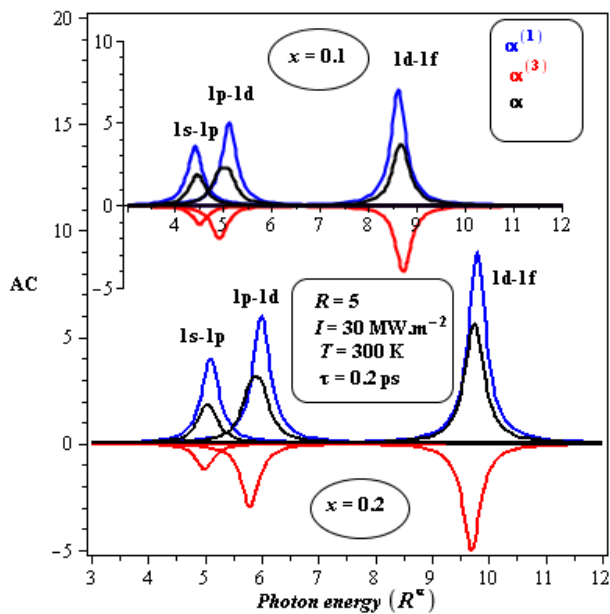


Fig. 3. The linear (blue), third-order nonlinear (red) and total (black) optical ACs (10^4 cm^{-1}) of 1s-1p, 1p-1d and 1d-1f transitions in (In,Ga)N/GaN SQD with an on-center impurity as a function of the incident photon energy. The *In*-composition is included.

The effect of the dot size on optical ACs of on-center hydrogenic impurity in (In,Ga)N SQD is shown on Figs. 2 and 3. On the one hand, it is readily seen that the optical ACs increase when the dot radius decreases. This result can be explained by the following fact: the optical ACs depend on the electron density in the dot which changes as $1/V$, and so it depends as $1/R^3$. On the other hand, a blue shift of the resonant peaks is obtained as a dot radius increases. This is caused by the increment in the energy difference between the two involved states as a consequence of the decrease of the dot radius. This effect is confirmed by the result obtained in Refs. [8, 14, 27-30].

Generally, our results are also in good agreement with those of several authors who concern different semiconductor materials [31-33]. Al-Khursan et al. [31] have studied the optical ACs of InGaAsP quaternary three-level QD system under wetting layer composition, pump power, quantum size and dephasing line-width effects. For spherical single electron Silicon (Si) quantum dots, Anchala et al. [32] have investigated the effects of incident intensity, dot radius and barrier height on photoabsorption process for intraband transitions. For GaAs/(Al,Ga)As SQD, Rezaei et al. [33] have presented the theoretical study of Simultaneous effects such as hydrogenic impurity, pump power and dot size on intersubband optical ACs using the Luttinger–Kohn effective mass equation. So, electronic structure and optical properties of the system are studied by means of the matrix diagonalization technique and compact density matrix approach, respectively. Incidentally, Baskoutas et al. [34,35] investigated the effects of the impurities, electric field, size

and optical intensity on optical ACs and refractive index changes in SQD and in an inverse parabolic QW.

It is interesting to mention that the results presented above can be affected when one takes into account of the large internal electric field due to piezoelectric (PZ) and spontaneous (SP) polarizations. SP polarization is feature of III-nitride wurtzite crystal which is an order of magnitude smaller than PZ polarization. This latter arises from strain due to lattice mismatch between (In,Ga)N (well) and GaN (barrier).

4. Conclusion

In summary, we have studied the influence of the dot size, the *In*-composition, the incident optical intensity and the presence of an on-center impurity on linear, third-order nonlinear and total intrasubband optical ACs of 1s-1p, 1p-1d and 1d-1f transitions in (In,Ga)N/GaN SQD. Our results revealed that:

- A critical value of the incident optical intensity is obtained splitting two intensity behaviors.
- The linear AC is not related to the incident optical intensity while this later has a great influence on the nonlinear AC.
- A blue shift of the resonant peaks is obtained by increasing (reducing) the *In*-composition (dot radius).

The present results are useful for further understanding the considerably effects of the mentioned parameters on the optical absorption of (In,Ga)N/GaN SQD. Due to the importance of this semiconductor material, we hope that this theoretical investigation may have consequences about practical application of electro-optical devices and optical communication.

Acknowledgement

The author would like to thank, Professor: A. Özmen from ‘‘ physics Department, Faculty of science, Selcuk University, Campus 42075, Konya, Turkey’’, for his help.

References

- [1] B. Çakir, A. Özmen, Ü. Atav, H. Üksel, Y. Yakar, *Int. J. Mod. Phys. C* **18**, 61 (2007).
- [2] B. Çakir, A. Özmen, Ü. Atav, H. Üksel, Y. Yakar, *Int. J. Mod. Phys. C* **19**, 599 (2008).
- [3] N. Aquino, *Adv. Quantum Chem.* **57**, 123 (2009).
- [4] I. F. I. Mikhail, I. M. M. Ismail, *Superlattices Microstruct.* **48**, 388 (2010).
- [5] D. Nasri, N. Sakkal, *Physica E* **42**, 2257 (2010).
- [6] H. El Ghazi, A. Jorio, *Physica B* **430**, 81 (2013).
- [7] H. El Ghazi, A. Jorio, I. Zorkani, *Physica B* **426**, 155 (2013).
- [8] G.H. Wang, K.X. Guo, *Physica E*, **28**, 14 (2005).
- [9] C. H. Liu, B. R. Xu, *Phys. Lett. A* **372**, 888 (2008).
- [10] C. J. Zhang, K. X. Guo, Z. E. Lu, *Physica E* **36**, 92

- (2007).
- [11] A. Özmen, Y. Yakar, B. Çakir, Ü. Atav, *Opt. Commn.* **282**, 3999 (2009).
- [12] Y. Yakar, B. Çakir, A. Özmen, *Commn. Theor. Phys.* **53**, 1185 (2010).
- [13] B. Çakir, Y. Yakar, A. Özmen, M. Ö. Sezer, M. Şahin, *Superlattices Microstruct.* **47**, 556 (2010).
- [14] Y. Yakar, B. Çakir, A. Özmen, *Opt. Commn.* **283**, 1795 (2010).
- [15] M. Şahin, *J. Appl. Phys.* **106**, 063710 (2009).
- [16] S. Shao, K. X. Guo, Z. H. Zhang, N. Li, C. Peng, *Superlattices Microstruct.* **48**, 541 (2010).
- [17] L. Zhang, Z. Yu, W. Yao, Y. Liu, H. Ye, *Superlattices Microstruct.* **48**, 434 (2010).
- [18] M. Kirak, S. Yilmaz, M. Şahin, M. Gençaslan, *J. Appl. Phys.* **109**, 094309 (2011).
- [19] G. Rezaei, M. R. K. Vahdani, B. Vaseghi, *Current Appl. Phys.* **11**, 176 (2011).
- [20] H. El Ghazi, A. Jorio, I. Zorkani, *Physica B* **410**, 49 (2013).
- [21] W. F. Xie, *Physica B*, **405**, 3436 (2010).
- [22] L. L. He, W. F. Xie, *Microstruct.* **47**, 266 (2010).
- [23] W. F. Xie, *Sol. State Commun.* **151**, 545 (2011).
- [24] H. El Ghazi, A. Jorio, *Physica B*, **429**, 42 (2013).
- [25] H. El Ghazi, A. Jorio, I. Zorkani, *Physica B* **427**, 106 (2013).
- [26] J. J. Shi, Z. Z. Gan, *J. Appl. Phys.* **94**, 407 (2003).
- [27] W. Xie, *Physica B* **403**, 4319 (2008).
- [28] W. Xie, *Commn. Theor. Phys.* **52**, 155 (2009).
- [29] W. Xie, *Opt. Commn.* **282**, 779 (2009).
- [30] J. Huang, Libin, *Phys. Lett. A* **372**, 4323 (2008).
- [31] A. H. Al-Khursan, M.K. Al-Khakani, K.H. Al-Mossawi, *Photonics Nanostruct: Fund. Appl.* **7**, 153 (2009).
- [32] Anchala, S. P. Purohit, K. C. Mathur, *Adv. Mat. Lett.* **3**, 498 (2012).
- [33] G. Rezaei, B. Vaseghi, N.A. Doostimotlagh, *Commn. Theor. Phys.* **57**, 485 (2012).
- [34] I. Karabulut, S. Baskoutas, *J. Appl. Phys.* **103**, 073512 (2008).
- [35] S. Baskoutas, C. Garoufalos, A.F. Terzis, *European Phys. J. B* **84**, 241 (2011).

*Corresponding author: hadghazi@gmail.com